

EFFECT OF VIRTUAL MASS FORCE ON PREDICTION OF PRESSURE CHANGES IN CONDENSING TUBES

by

Hamid SAFFARI* and Nemat DALIR

LNG Research Laboratory, School of Mechanical Engineering,
Iran University of Science and Technology, Narmak, Tehran, Iran

Original scientific paper
DOI: 10.2298/TSCI1202613S

Three-fluid model is used to calculate the pressure drops in a vertical pipe with the annular flow pattern for condensing steam. The three-fluid models are based on the mass, momentum, and energy balance equations for each of the fluid streams in the annular flow. There are discrepancies between predictions of three-fluid model for pressure drops and the experimental data for pressure drops when using the available correlations for steam-film interfacial friction. The correlation by Stevanovic et al. provides good match with experimental data, but it does not take into account some important factors affecting the pressure drops in its three-fluid model. One of these significant factors which is considered in the three fluid model used in the present paper is virtual mass (added mass) force term. Inclusion of the virtual mass force improves the pressure drop predictions such that they agree much better with the experiments.

Key words: *three-fluid model, annular flow, condensation, pressure change, virtual mass force*

Introduction

The phenomenon of condensation of steam inside vertical pipes takes place in air heaters in steam boilers, air-cooled condensers, and steam condensers within the passive systems of nuclear power plants. In an air-cooled condenser, for instance, the drained condensate in the vertical condensing pipe must be removed from pipe outlet header to the condensate line, which requires adequate pressure drop along the steam flow in the pipe. The prediction of this required pressure drop is very significant in designing an air-cooled condenser. If the required pressure drop is not provided, the liquid condensate will gather at outlet sections of the condensing pipe and decrease of condensation surface will result. Moreover, in order for the condenser to operate reliably, the steam flow must have a uniform distribution among parallel pipes. This uniform distribution of steam flow among parallel pipes can be assured only when the exact values of pressure drop along the condensing pipe are known.

The three-fluid models are often used for the prediction of pressure drops in the case of boiling or adiabatic flows of steam, liquid film, and entrained droplets in vertical or inclined pipes. But in the present paper the three-fluid model is used to predict the pressure drop inside a

* Corresponding author; e-mail: saffari@iust.ac.ir

vertical pipe with annular flow pattern of steam, liquid film, and droplets. The previous studies investigating the three-fluid model for annular flow have all concluded that results of the three-fluid model depend heavily on the type of correlations used for the calculation of interfacial transfer of mass and momentum between the fluids. They have also particularly emphasized on the effect of correlations used for droplet deposition and entrainment, and on the effect of closure relation used for steam-liquid film interfacial friction coefficient on the three-fluid model results. In the present study, the capability of the three-fluid model to calculate pressure drops in the annular condensing flow of steam, film, and droplets in vertical pipes is examined for the available experimental circumstances. The annular flow parameters are analyzed and some of the available correlations for steam-film interfacial friction coefficient are examined. A correlation for the interfacial friction on the wavy liquid film surface, proposed by Stevanovic *et al.* [1], suggests that the variation of steam and liquid film density with pressure has an effect on the friction in steam-liquid interface. Here this correlation is modified by taking the virtual mass force term into account. The results obtained using the new modified correlation has better match with the experimental results compared to available correlations.

Figure 1 demonstrates a pure and saturated steam flows inside a vertical pipe. The steam is condensed completely in the pipe by applying cooling heat flux to the pipe surface. As condensation begins, annular flow pattern forms inside the pipe such that there is flowing steam

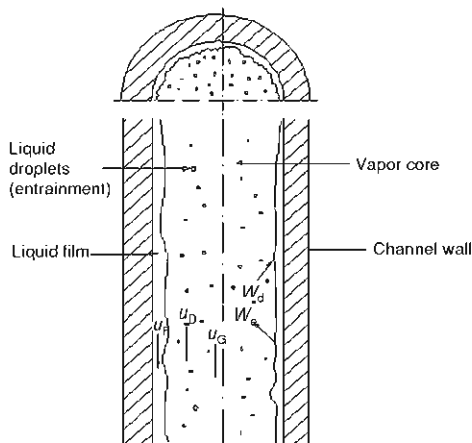


Figure 1. Three-fluid modelling in vertical annular two-phase flow

at the pipe core, liquid film at the pipe surface and droplets flowing along with steam which are entrained from the liquid film. Therefore, the entrainment and deposition of liquid droplets also happen. Pressure drops in the pipe are calculated by developing a three-fluid model. However, there are discrepancies between predictions of three-fluid model and the experimental data for pressure drops when using the available correlations for steam-film interface friction. The correlation by Stevanovic *et al.* [1] provides good match with experimental data, but it does not take into account some important factors affecting the pressure drop. One of these significant factors which is considered in the three fluid model used in the present paper is virtual mass force term. Inclusion of the virtual mass force improves the pressure drop predictions such that they agree much better with the experiments.

Modeling approach

The governing equations of condensation of steam in a vertical pipe with annular flow for the three-fluid model are nine equations which include mass conservation equations (continuity equations) for three fluids of the three-fluid model, *i. e.*, gas, liquid film, and entrained droplets, momentum conservation equations (force balance equations) for gas, liquid film, and entrained droplets, and energy conservation equations (first law of thermodynamics) for gas, liquid film, and entrained droplets. It should be noted that the governing equations are steady 1-D equations for which only spatial dimension of the problem is upward along vertical

pipe. The tenth equation for the problem of condensing vertical pipe is obtained by summing volume fractions of gas, liquid film, and entrained droplets which become one. Using these ten obtained equations, ten unknowns of the problem are obtained. These ten unknowns that are sometimes called state variables consist of nine variables for enthalpy, volume fraction, and velocity for three-fluids of gas, liquid film, and droplets, and a variable for pressure. The mass, momentum and energy transfer between pairs of gas, liquid film, and entrained droplets and also between pipe surface and liquid film are calculated using proper closure equations.

By performing some algebraic manipulation on ten governing equations of the problem, these equations are converted to ten first order non-homogeneous ordinary differential equations, which are coupled together as a system of ordinary differential equations (ODE). This system of ODE is a stiff system because variable of volume fraction varies only between zero and one while variable of pressure can vary in a very large domain from zero to a few mega-Pascals. It should be noted that having a stiff ODE system is the common feature of all condensation and also evaporation problems. Two of MatLab built-in stiff ODE solvers including ode23s and ode15s are used to solve the present stiff condensation problem of three-fluid model, for which variable values at inlet of pipe are the initial conditions.

It should be noted that in the three-fluid model for annular flow, the pressure is assumed constant in each cross-section. Also it should be noted that in the three-fluid model, the velocity of each of the three-fluids is constant in its own cross-section and is considered to be the mean velocity of the fluid. Thus there is no need for grid and meshing in the cross-section and of course no need for computational fluid dynamics methods. Note that the velocity of each fluid is constant in its own cross-section but it varies with longitudinal position, and also, in general, it is different from the velocity of the two other fluids in the same longitudinal position.

It is assumed that the vapor remains saturated everywhere because the vapor-side thermal resistance can be neglected (therefore for the vapor thermo-physical properties, saturated vapor properties can be used from thermodynamic property tables), but the liquid film will be slightly sub-cooled. It should be noted that the thermo-physical properties of the liquid film and entrained droplets are the same (*i. e.* $\rho_2 = \rho_3$ and $\mu_2 = \mu_3$).

Governing equations

The mass, momentum and energy conservation equations for the steady 1-D flow of three fluids including gas, liquid film and droplets are as follows [2]:

– *mass conservation equations*

$$\text{gas} \quad \frac{d(\alpha_1 \rho_1 u_1)}{dx} = (\Gamma_{21} - \Gamma_{12}) + (\Gamma_{31} - \Gamma_{13}) \quad (1)$$

$$\text{liquid film} \quad \frac{d(\alpha_3 \rho_3 u_3)}{dx} = (\Gamma_{13} - \Gamma_{31}) - a_{12}(W_d - W_e) \quad (2)$$

$$\text{droplets} \quad \frac{d(\alpha_2 \rho_2 u_2)}{dx} = (\Gamma_{13} - \Gamma_{31}) + a_{12}(W_d - W_e) \quad (3)$$

– *momentum conservation equations*

$$\text{gas} \quad \frac{d(\alpha_1 \rho_1 u_1^2)}{dx} + \alpha_1 \frac{dp}{dx} = (-a_{12} \tau_{12} - a_{13} \tau_{13}) + (\Gamma_{21} u_2 - \Gamma_{12} u_1) + (\Gamma_{31} u_3 - \Gamma_{13} u_1) - \alpha_1 \rho_1 g \sin \theta + F_{VM} \quad (4)$$

$$\text{liquid film} \quad \frac{d(\alpha_2 \rho_2 u_2^2)}{dx} + \alpha_2 \frac{dp}{dx} = (a_{12} \tau_{12} - a_{2W} \tau_{2W}) + (\Gamma_{12} u_1 - \Gamma_{21} u_2) + \quad (5)$$

$$+ a_{12} (W_d u_3 - W_e u_2) - \alpha_2 \rho_2 g \sin \theta$$

$$\text{droplets} \quad \frac{d(\alpha_3 \rho_3 u_3^2)}{dx} + \alpha_3 \frac{dp}{dx} = a_{13} \tau_{13} + (\Gamma_{13} u_1 - \Gamma_{31} u_3) - \quad (6)$$

$$- a_{12} (W_d u_3 - W_e u_2) - \alpha_3 \rho_3 g \sin \theta - F_{VM}$$

– energy conservation equations

$$\text{gas} \quad \frac{d(\alpha_1 \rho_1 u_1)}{dx} = (\Gamma_{21} - \Gamma_{31}) h_{g,sat} - (\Gamma_{12} + \Gamma_{13}) h_{l,sat} \quad (7)$$

$$\text{liquid film} \quad \frac{d(\alpha_2 \rho_2 h_2 u_2)}{dx} = \Gamma_{12} h_{l,sat} - \Gamma_{21} h_{g,sat} + a_{12} (W_d h_3 - W_e h_2) + \dot{q}_{V,2} \quad (8)$$

$$\text{droplets} \quad \frac{d(\alpha_3 \rho_3 h_3 u_3)}{dx} = \Gamma_{13} h_{l,sat} - \Gamma_{31} h_{g,sat} + a_{12} (W_d h_3 - W_e h_2) \quad (9)$$

where we have $h_{l,sat} = h_l(p)$ and $h_{g,sat} = h_g(p)$.

The volume balance equation is:

$$\alpha_1 + \alpha_2 + \alpha_3 = 1 \quad (10)$$

By doing some algebraic manipulation as performed in [1], eqs. (1) to (10) can be cast into ten first order ordinary differential equations (ODE), *i. e.*, the system of conservation equations is transformed in a form suitable for the numerical integration. The system of first order ODE is solved using MatLab built-in functions for ODE integration. MatLab ODE integrators consider system of equations as an initial-value problem, therefore initial conditions should be provided for the system of ten first order ODE. Here the initial conditions provided for the system of ODE are the values of ten unknown parameters ($h_1, h_2, h_3, \alpha_1, \alpha_2, \alpha_3, u_1, u_2, u_3$, and p) and at the inlet of the pipe ($h_{1,0}, h_{2,0}, h_{3,0}, \alpha_{1,0}, \alpha_{2,0}, \alpha_{3,0}, u_{1,0}, u_{2,0}, u_{3,0}$, and p_0).

Constitutive relations and comments

Sugawara [3] estimates the entrainment rate W_e from a correlation as follows:

$$W_e = 1.07 \frac{u_1 \mu_3 \tau_{21} \Delta h_{eq}}{\sigma^2} \left(\frac{\rho_3}{\rho_1} \right)^{0.4} \quad \text{where} \quad \Delta h_{eq} = \begin{cases} k_s, & \text{Re}_1 > 10^5 \\ k_s [2.136 \log(\text{Re}_1) - 9.68], & \text{Re}_1 < 10^5 \end{cases} \quad (11)$$

$$k_s = 0.6\delta + 21.7 \cdot 10^3 \delta^2 - 38.8 \cdot 10^6 \delta^3 + 55.6 \cdot 10^9 \delta^4$$

where $\delta = 0.5D[1 - (1 - \alpha_2)^{1/2}]$ is the mean liquid film thickness.

At each position of the pipe the deposition rate W_d can be calculated as $W_d = k_d C$. Sugawara [3] uses the following correlations to calculate the deposition constant, k_d , and concentration of droplets in gas, C :

$$k_d = 0.01 u_1 \left(\frac{C}{\rho_1} \right)^{-0.5} \text{Re}_1^{-0.2} \text{Sc}_1^{-2/3} \quad C = \frac{1}{\frac{\dot{m}_1 u_3}{\dot{m}_3 \rho_1 u_1} + \frac{1}{\rho_3}} \quad (12)$$

The wall-liquid film shear stress is defined as:

$$\tau_{2W} = f_{2W} \left[\frac{1}{2} \rho_2 (u_2)^2 \right] \quad (13)$$

where the wall-liquid film interfacial friction coefficient is [4]:

$$f_{2W} = \frac{C}{\text{Re}_2^n}, \quad \begin{cases} C = 16, n = 1, \text{ if } \text{Re}_2 \leq 1600 \\ C = 0.079, n = 0.25, \text{ if } \text{Re}_2 > 1600 \end{cases} \quad (14)$$

The liquid film Reynolds number is $\text{Re}_2 = \rho_2 u_2 D_{h,2} / \mu_2$, and $D_{h,2} = D \alpha_2$ is the hydraulic diameter of liquid film flow.

The shear stress between gas phase and droplets is defined as:

$$\tau_{13} = \frac{1}{8} C_D \rho_1 (u_1 - u_3)^2 \quad (15)$$

Clift *et al.* [5] defines the drag coefficient between gas and droplets, C_D , as:

$$C_D = \frac{1}{\text{Re}_D} (24 + 3.6 \text{Re}_D^{0.867}) + \frac{0.42}{1 + 4.25 \cdot 10^4 \text{Re}_D^{-1.16}} \quad (16)$$

and $\text{Re}_D = \rho_1 |u_1 - u_3| D_D / \mu_1$ is the entrained droplets Reynolds number.

Mean droplet diameter can be calculated as [6]:

$$D_D = \begin{cases} 10^{-4} \text{ m, for } Y \leq 10^{-4} \\ Y, \text{ for } 10^{-4} < Y < 3 \cdot 10^{-3}; \text{ where } Y = \frac{0.799\sigma}{\rho_1 (u_1 - u_3)^2} \\ 3 \cdot 10^{-3}, \text{ for } Y \geq 3 \cdot 10^{-3} \end{cases} \quad (17)$$

The shear stress between liquid film and gas phase is defined as:

$$\tau_{12} = f_{12} \left[\frac{1}{2} \rho_1 (u_1 - u_2)^2 \right] \quad (18)$$

Many correlations have been used for gas phase-liquid film interfacial friction coefficient in the literature [1, 7-9]. Some of these correlations used in the present paper are:

– modified Wallis correlation [7]

$$f_{12} = \frac{1}{\text{Re}_1^{0.25}} \left(0.079 + 23.7 \frac{\delta}{D} \right) \quad (19)$$

where $\text{Re}_1 = \rho_1 u_1 D_{h,13} / \mu_1$ is the gas phase flow Reynolds number, and $D_{h,13} = D(1 - \alpha_2)^{1/2}$ is the hydraulic diameter of the gas phase;

– Levitan correlation [8]

$$f_{12} = \left(\frac{\rho_2}{\rho_1} \right)^{0.4} \left(0.001 + 0.3 \frac{\delta}{D} \right) \quad (20)$$

– Alipchenkov *et al.* correlation [9]

$$f_{12} = \frac{0.25}{(1.8 \log \text{Re}_1 - 1.64)^2} + \frac{3\delta}{2D} \quad (21)$$

– Stevanovic *et al.* correlation [1]

$$f_{12} = \frac{0.079}{\text{Re}_1^{0.25}} + 46.35 \frac{\delta}{D} \left(\frac{\rho_1}{\rho_2} \right)^{0.8} \quad (22)$$

Condensation and evaporation rates. Non-equilibrium relaxation method is used to calculate the condensation and evaporation rates, in which the volumetric condensation and evaporation rates are obtained as [10]:

– condensation rate

$$\Gamma_{1k} = \frac{\alpha_k \rho_k}{\tau_e} \frac{h_f - h_k}{h_{fg}} \quad \text{for } h_f > h_k, \quad k = 2, 3 \quad (23)$$

$$\Gamma_{1k} = 0 \quad \text{for } h_k \leq h_f$$

– evaporation rate

$$\Gamma_{k1} = \frac{\alpha_k \rho_k}{\tau_e} \frac{h_k - h_f}{h_{fg}} \quad \text{for } h_k > h_f, \quad k = 2, 3 \quad (24)$$

$$\Gamma_{k1} = 0 \quad \text{for } h_k \leq h_f$$

where $\tau_c = \tau_e = 0.01 + 0.99\alpha_1$ are condensation and evaporation relaxation times, $h_{fg} = h_{fg}(p)$ is the condensation or evaporation latent enthalpy, and $h_f = h_f(p) = h_{1,\text{sat}}(p)$ – the liquid saturation enthalpy.

The cross-section of pipe flow is $A = \pi D^2/4$, liquid film-wall perimeter is $S_{2W} = \pi D$, and liquid film-gas perimeter is $S_{12} = \pi D(1 - \alpha_2)^{1/2}$. Therefore the liquid film-wall, liquid film-gas and droplets-gas interfacial area concentrations are obtained as [11]:

$$a_{2W} = \frac{S_{2W}}{A} = \frac{4}{D}, \quad a_{12} = \frac{S_{12}}{A} = \frac{4\sqrt{1-\alpha_2}}{D}, \quad a_{13} = 6 \frac{\alpha_3}{D_D} \quad (25)$$

Virtual mass (added mass) force term. The correction considered in the present paper for the three-fluid model prediction of pressure changes in condensing vertical pipes assuming annular flow is the introduction of virtual mass (added mass) force term. Therefore, the new modified three-fluid model presented in the present paper is the three-fluid model using Stevanovic *et al.* [1] correlation for steam-liquid film interfacial friction coefficient with a correction, *i. e.*, introduction of added mass force term. The added mass force takes place if there is a continuous phase and a discontinuous phase such that the discontinuous phase motion accelerates the continuous phase. A simple and widely used expression for virtual mass force in steady one-dimensional separated flow which is used in the written MatLab code is [12]:

$$F_{VM} = -C_{VM} \left[u_1 \frac{\partial u_1}{\partial x} - u_3 \frac{\partial u_3}{\partial x} \right] \quad (26)$$

Watanabe *et al.* [13] have suggested $C_{VM} = C' \alpha_1 (1 - \alpha_1) \rho$, with $C' \approx 1$ and $\rho = \alpha_1 \rho_1 + \alpha_2 \rho_2$.

The exact form of the virtual mass force term is only known from theory for some simple and idealized conditions. The general form of virtual mass force in two-phase flow has been a subject of considerable discussion. Drew *et al.* [14] derived a general form for the force term based on the argument that the force must be objective (frame independent). Their proposed general form includes regime-dependent parameters that can only be obtained from theory for some idealized configurations. One suggested expression for the virtual mass force is from Ishii *et al.* [15]:

$$\vec{M}_{IV,d} = -\frac{1}{2}\alpha_3 \frac{1+2\alpha_3}{1-\alpha_3} \rho_1 \left[\frac{D_d}{Dt} (\vec{u}_3 - \vec{u}_1) - (\vec{u}_3 - \vec{u}_1) \nabla \vec{u}_1 \right] \quad (27)$$

where material derivative is defined as $D_d/Dt = \partial/\partial t + (\vec{u}_3 \cdot \nabla)$.

The steady 1-D form of $\vec{M}_{IV,d}$ becomes:

$$F_{VM} = -\frac{1}{2}\alpha_3 \frac{1+2\alpha_3}{1-\alpha_3} \rho_1 \left[u_3 \frac{\partial(u_3 - u_1)}{\partial x} - (u_3 - u_1) \frac{\partial u_1}{\partial x} \right] \quad (28)$$

In terms of magnitude, F_{VM} is significant only if the gas phase is dispersed, and only in rather extreme flow acceleration conditions (*e. g.*, choked flow). Despite the insignificant quantitative effect, however, the virtual mass term is important because it modifies the mathematical properties of the momentum conservation equation and improves the numerical stability of the conservation equation set.

Results and discussion

The experimental data for pressure drops in condensing pipe are taken from Kreydin *et al.* [16]. They used a condensing pipe with 0.0132 m diameter and 2.93 m length. As the first step, the total pressure drops are computed at various total mass fluxes. The total mass flux (G) is varied here from zero to 500 kg/m²s. A uniform condensing heat flux is used on the tube surface in order to condensate the steam. For example, heat fluxes of -68 W/cm², and -112 W/cm² are required to condensate the steam with mass fluxes of 300 kg/m²s, and 500 kg/m²s, respectively. It should be noted that at the tube entrance there is pure saturated steam and at the tube exit there are sub-cooled water and saturated steam. The tube has a constant length, therefore the condensing heat flux changes proportionally with the mass flux.

Figure 2 compares the predicted values of pressure drops by using the new modified three-fluid model with the measured pressure drops of Kreydin *et al.* [16]. In fig. 2, the horizontal axis is the total mass flux and the steam inlet pressure is 1.08 MPa. It should be noted that here the total pressure drop is the difference between outlet pressure and inlet pressure. It can be observed from fig. 2 that better match with the measured pressure drops of Kreydin *et al.* [16] is provided by the new modified three-fluid model (correlation of Stevanovic

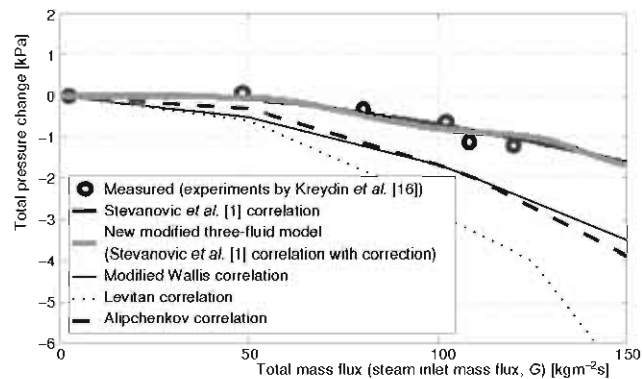


Figure 2. New three-fluid model predictions (Stevanovic *et al.* [1] correlation with correction) compared with measured data by Kreydin *et al.* [16] (steam inlet pressure is 1.08 MPa)

et al. [1] corrected by introducing the virtual mass force term) compared to other correlations.

The volume fraction of condensate (liquid film + entrained droplets), $\alpha_2 + \alpha_3$, is shown in terms of the distance from the tube inlet for the steam inlet pressure of 1.08 MPa and different total mass fluxes in fig. 3. It can be seen that the condensate volume fraction increases along the tube length. The condensate volume fraction does not become more than 0.4, in fact for usual

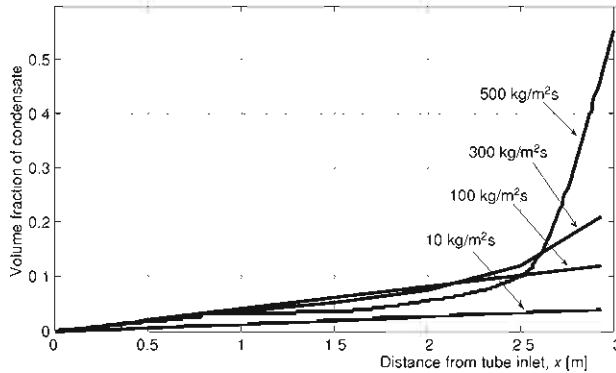


Figure 3. Condensate volume fraction change from the inlet to the outlet of vertical condensing tube for different total mass fluxes (steam inlet mass fluxes) (steam inlet pressure is 1.08 MPa)

changes linearly with tube length. For higher mass fluxes (300 and 500 kg/m²s), the condensate volume fraction changes linearly with tube length, but at the end lengths of the tube the condensate volume fraction increases rapidly and non-linearly with tube length. These rapid and non-linear changes in condensate volume fraction, for higher mass fluxes, shows that at the end lengths of the tube the flow pattern changes from annular flow to slug flow, and consequently the use of the three-fluid model is not justified.

The new three-fluid model has also been used to simulate the steam condensing downward flow of Kim *et al.* [17]. Here the tube diameter is $D = 0.0462$ m and the tube length is $L = 1.8$ m. The saturated steam inlet pressure changes from 1 MPa to 7 MPa. The condensation of steam takes place from tube inlet to outlet. The cooling (or condensing) heat flux is constant (uniform) along the condensing tube. The calculated (by the new three-fluid model) and measured (experiments by Kim *et al.* [17]) total pressure changes are plotted against the steam inlet pressure (P_0), in a constant total mass flux, fig. 4. It can be seen that the total pressure change (total pressure drop) increases when the steam inlet pressure increases. When the inlet pressure

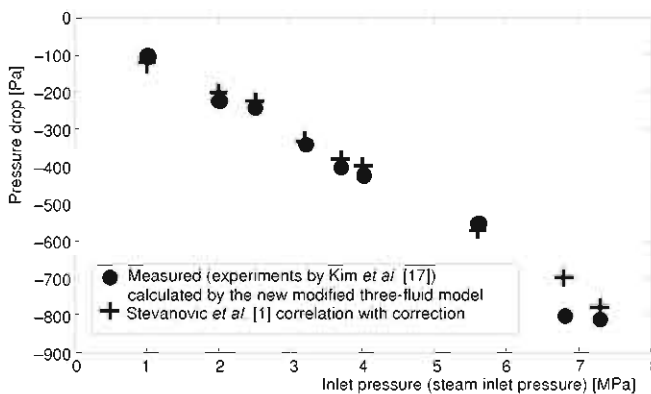


Figure 4. Pressure drops in a condenser tube (new three-fluid model predictions compared with experimental data of Kim *et al.* [17])

values of mass fluxes, the condensate volume fraction does not even reach 0.2. Only for higher mass fluxes (which also means higher condensing heat fluxes) the condensate volume fraction reaches values higher than 0.2. For $\alpha_2 + \alpha_3 < 0.2$ or 0.3, the annular flow pattern holds along the whole tube length. Therefore the pre-assumption of annular flow and the use of three-fluid model are justified.

For usual values of total mass fluxes (*i. e.* 10 and 100 kg/m²s), the condensate volume fraction

increases, the total pressure drop increases almost linearly. It should be noted that although the total pressure drop of condensing steam flow inside vertical tubes increases by the increase of steam inlet pressure, this increase is not considerable. Figure 4 shows that when the inlet pressure increases about 10 bar, the total pressure drop increases about 0.001 bar. Therefore, it can be concluded that the pressure drop inside condensing vertical tubes is not affected considerably by the changes of steam inlet pressure.

Conclusions

Three-fluid model is used to calculate the pressure drops in annular flow inside condensing steam pipes. There are discrepancies between predictions of three-fluid model for pressure drops and the experimental data for pressure drops when using the available correlations for steam-film interface friction. The correlation by Stevanovic *et al.* [1] provides good match with experimental data, but it does not take into account an important factor affecting the pressure drops in its three-fluid model, namely virtual mass force term, which is considered in the three fluid model used in the present paper.

The mass, momentum, and energy conservation equations for steady 1-D flows of the three fluids, *i. e.*, gas, liquid film, and droplets are written along with the volume balance equation, which make a total of ten equations for calculating ten unknowns. Using proper closure equations, the mass, momentum and energy transfer across fluid interfaces are also treated.

By doing some algebraic manipulation, the conservation equations and volume balance equation are cast into ten first order ODE. The system of first order ODE is solved using MatLab built-in functions for ODE integration, *i. e.*, ode23s and ode15s. Initial conditions are provided for the system of ten first order ODE which here are the values of ten unknown parameters at the inlet of the pipe. Some of the results obtained can be summarized as follows.

- The new modified three-fluid model (Stevanovic *et al.* [1] correlation with correction – introduction of virtual mass force term) provides better agreement with measured data compared to other correlations.
- The condensate volume fraction increases along the tube length. For usual values of mass fluxes, the condensate volume fraction does not even reach 0.2. Only for higher mass fluxes, the condensate volume fraction reaches values higher than 0.2. For $\alpha_2 + \alpha_3 < 0.2$ or 0.3, the annular flow pattern holds along the whole tube length, and therefore the pre-assumption of annular flow and the use of three-fluid model are justified.
- The new three-fluid model has also been used to simulate the steam condensing downward flow of Kim *et al.* [17]. The total pressure drop increases when the steam inlet pressure increases.

Nomenclature

A	– channel cross-sectional area, [m ²]	P	– pressure, [Pa]
a	– interfacial area concentration, [m ⁻¹]	q_v	– volumetric heat flux
C_D	– drag coefficient, [–]	Re	– Reynolds number ($= \rho U l / \mu$), [–]
D	– diameter, [m]	S	– perimeter, [m]
F_{VM}	– virtual mass force, per unit mixture volume, [Nm ⁻³]	t	– time, [s]
f	– friction coefficient, [–]	u	– velocity, [ms ⁻¹]
G	– mass flux [kgm ⁻² s ⁻¹]	W_d	– deposition rate of entrained droplets, [kgm ⁻² s ⁻¹]
g	– gravitational constant, [ms ⁻²]	W_e	– droplets entrainment rate, [kgm ⁻² s ⁻¹]
h	– specific enthalpy, [Jkg ⁻¹]	We	– Weber number ($= \rho U^2 l / \sigma$), [–]
h_{fg}	– latent heats of vaporization, [Jkg ⁻¹]	x	– co-ordinate, [m]
k	– thermal conductivity, [Wm ⁻¹ K ⁻¹]	<i>Greek symbols</i>	
L	– length, [m]	α	– volume fraction, [–]
M	– source terms in balance equations, [–]	Γ	– evaporation/condensation rate, [kgm ⁻³ s ⁻¹]
M_{IV}	– virtual mass force term, [Nm ⁻³]	δ	– liquid film thickness, [m]
m	– mass, [kg]		

θ	– angle of tube inclination, [rad]	F	– film
μ	– dynamic viscosity, [$\text{kgm}^{-1}\text{s}^{-1}$]	G	– gas
ν	– kinematic viscosity, [m^2s^{-1}]	h	– hydraulic parameter
ρ	– density, [kgm^{-3}]	k	– phase indicator
σ	– surface tension, [Nm^{-1}]	W	– wall
τ	– shear stress, [Nm^{-2}]	o	– initial conditions
τ_e	– evaporation relaxation time, [s]	1	– gas
τ_c	– condensation relaxation time, [s]	2	– liquid film
Subscripts		3	– entrained droplets
D	– droplet		

References

- [1] Stevanovic, V. D., et al., Three-Fluid Model Predictions of Pressure Changes in Condensing Vertical Tubes, *Int. J. of Heat and Mass Transfer*, 51 (2008), 15-16, pp. 3736-3744
- [2] Jayanti I. S., Valette, M., Prediction of Dryout and Post-Dryout Heat Transfer at High Pressures Using a One-Dimensional Three-Fluid Model, *Int. J. of Heat and Mass Transfer*, 47 (2004), 22, pp. 4895-4910
- [3] Sugawara, S., Miyamoto, Y., FIDAS: Detailed Sub-Channel Analysis Code on the Three-Fluid and Three-Field Model, *Nuclear Engineering and Design*, 120 (1990), 2-3, pp. 147-161
- [4] White, F. M., Viscous Fluid Flow, McGraw-Hill, New York, USA, 1991
- [5] Clift, R., Grace, J. R., Weber, M. E., Bubbles, Drops and Particles, Academic Press, New York, USA, 1978
- [6] Sugawara, S., Droplet Deposition and Entrainment Modeling Based on the Three-Fluid Model, *Nuclear Engineering and Design*, 122 (1990), 1-3, pp. 67-84
- [7] Wallis, G. B., One-Dimensional Two-Phase Flow, McGraw-Hill, New York, USA, 1969
- [8] Levitan, L. L., Dry-Out in Annular-Dispersed Flow, Advances in Thermal-Hydraulics of Two-Phase Flows in Energy Plants (in Russian), Nauka, Moscow, 1987
- [9] Alipchenkov, et al., Three-Fluid Model of Two-Phase Dispersed-Annular Flow, *Int. J. of Heat and Mass Transfer*, 47 (2004), 24, pp. 5323-5338
- [10] Downar-Zapolski, Z., et al., The Non-Equilibrium Relaxation Model for One-Dimensional Flashing Liquid Flow, *Int. J. of Multiphase Flow*, 22 (1996), 3, pp. 473-483
- [11] Hazuku, T., et al., Interfacial Area Concentration in Annular Two-Phase Flow, *Int. J. of Heat and Mass Transfer*, 50 (2007), 15-16, pp. 2986-2995
- [12] Ghiaasiaan, S. M., Two-Phase Flow, Boiling and Condensation in Conventional and Miniature Systems, 1st ed., Cambridge University Press, Cambridge, UK, 2008
- [13] Watanabe, T., et al., The Effect of Virtual Mass Force Term on the Numerical Stability and Efficiency of System Calculations, *Nucl. Eng. Design*, 120 (1990), 2-3, pp. 181-192
- [14] Drew, D. A., Cheng, L. Y., Lahey, R. T., The Analysis of Virtual Mass Effect in Two-Phase Flow, *Int. J. Multiphase Flow*, 5 (1979), 4, pp. 233-242
- [15] Ishii, M., Mishima, K., Two-Fluid Model and Hydrodynamic Constitutive Relations, *Nucl. Eng. Design*, 82 (1984), pp. 2-3, pp. 107-126
- [16] Kreydin, B. L., Kreydin, I. L., Lokshin, V. A., Experimental Research of the Total Pressure Drop in the Condensing Steam Downward Flow Inside a Vertical Tube (in Russian), *Thermal Engineering*, 32 (1985), 7, pp. 42-43
- [17] Kim, S. J., No, H. C., Turbulent Film Condensation of High Pressure Steam in a Vertical Tube, *Int. J. Heat Mass Transfer*, 43 (2000), 21, pp. 4031-4042

Paper submitted: October 6, 2010

Paper revised: April 14, 2012

Paper accepted: May 5, 2012